PHY324: Comparison of the classical and quantum models of the photoelectric effect by reproducing the results of Philip Lenard's experiment, measuring the relation between the frequency and intensity of incident light and the corresponding photocurrent and stopping voltage required

By: Gurmanjot Singh and Aran Wade

Due: 19 March 2023

1 Abstract

In this paper, we discuss the findings of a simplified version of Philip Lenard's famous experiment on the photoelectric effect. Particularly, we measure how the stopping voltage of our cathode changes with the frequency of incident light on it. Using the established linear relation between the two, we compute a value for Planck's constant $h = (4.6491 \pm 0.0006) \times 10^{-34}$ Js, the work function of the cathode's metal $E_0 = (1.5655 \pm 0.0003) \times 10^{-19}$ J, and the threshold frequency $f_0 = (3.2850 \pm 0.0004) \times 10^{14}$ Hz in the semiclassical model. Using the fact that there is a nonzero frequency for which no photocurrent is generated, along with the result of additional measurements that the stopping voltage does not depend significantly on the intensity of incident light for a range of settings, as well as a large discrepancy between the classical delay time of $T \approx 0.9 \pm 0.3$ s in the response in comparison to the much smaller measured actual delay time of $T_a = (8.5 \pm 0.3) \times 10^{-5}$ s, we conclude that the classical theory does not sufficiently model this effect. This motivates considering the semiclassical theory of electromagnetism, which coincides much better with our results and calls for extensions into more sophisticated experimentation into this field.

2 Introduction and Theory

The study of the photoelectric effect was pivotal in understanding the motivations behind the model for quantized light. When a cathode in a circuit is subjected to light coming from an external source, bound electrons in the metal absorb a certain amount of energy from the incident radiation and is released into the circuit as photoelectrons, producing a current, called a photocurrent [1].

Classical electromagnetic theory models that the electron continuously absorbs the electromagnetic waves over time up to a certain threshold energy, E_0, called the work function of the metal, past which the electron discharges from the metal. This hence predicts that all frequencies and intensities of incident light should produce a photocurrent, as bound electrons should eventually absorb enough energy to bypass the work function barrier. This also suggests there should be a time delay for the photocurrent to appear, dependent on the frequency and intensity of the radiation, as the time taken for the first electrons to receive enough energy for release. The strength of the photocurrent should also depend continuously on the intensity squared and frequency, as they are proportional to the energy and so decide the rate of energy deposition.

On the other hand, Einstein proposed that light was instead quantized as particles called photons, of a particular frequency f and energy $E = hf$, where h is Planck's constant. This semiclassical model predicts that the electron only absorbs photons that have enough energy to eject it–that is, with frequency f for which $hf \geq E_0$. This should produce a photocurrent in the circuit much faster, as now there would be marginal delay in the electron absorbing a sufficient photon to escape. Moroever, if the frequency of incident light is not high enough for the individual photons to be absorbed, we should expect no photocurrent–in the case of $f < E_0/h$. The threshold frequency is thus $f_0 = E_0/h$, as $f \geq f_0$ is required to allow the photocurrent to flow.

Note that this photocurrent is expected to no longer depend on the frequency other than the jump at f_0. On the other hand, it should still increase with the intensity, which corresponds to the density of photons in the radiation per unit area and so the number of electrons that are ejected per unit time increases. Given the incident photon's frequency f, we know that–if the electron is released–it will have residual kinetic energy $hf - E_0$. To resist this, we can apply an opposing potential difference ΔV in the circuit using a potentiometer, which would reduce the kinetic energy and the photocurrent.

If we make this sufficiently large, we can completely negate the photocurrent, which is the special voltage $\Delta V = V_s$ that completely cancels the kinetic energy of the discharged electron, which means that $eV_s = hf - E_0 = h(f - f_0)$, where e is the charge of the electron. The relation:

$$V_s = mf + b \tag{1}$$

is predicted, where $m = h/e$ and $b = -E_0/e$, for $f > f_0$, and $V_s = 0$ otherwise. When we measure this stopping voltage for various frequencies of light incident on a phototube, we can perform a linear fit with this relation on m and b. If the semiclassical model of light is correct, we expect this to be a good fit, which we will do in this lab. We see that if we know the electron charge e, we can then calculate Planck's constant $h = em$ and the work function $E_0 = eb$, which then gives us the cutoff frequency as $f_0 = E_0/h = b/m$.

The intensity L of the incident light on the phototube corresponds to the incident power per unit area. In the semiclassical model, within a time interval t, this is equal to the rate of absorption of the total energy from N photons per area A of the phototube, or $L = hNf/(At)$ if this is assumed to

be uniform. Since since the rate of absorption N/t is also the rate of photoelectron ejection, which produces a photocurrent $I = eN/t$, we get a linear relationship:

$$I = aL \tag{2}$$

between the photocurrent and the intensity if we fix the frequency, where $a = \frac{eA}{hf}$ [6]. Classically, the intensity also corresponds to the field energy density per unit time, so we would also expect a similar relation. The difference comes in the stopping voltages for each intensity–the semiclassical model predicts that the energy of the photons do not increase with intensity, just the number, so the kinetic energy of the ejected electrons due to photons should not increase with intensity–if we assume that photons only interact once during the ejection. Mainly, the stopping voltage should not change with the intensity if the semiclassical model is true.

On the other hand, the classical model has the energy of the electrons depend on the intensity as with the frequency, so we would expect an upwards linear trend with the stopping voltage, as more kinetic energy would require a larger opposing potential to stop it. By looking at the relationship of L and V_s, we have another metric to decide which one of these models are better suited.

Finally, as mentioned before, the semiclassical model predicts nearly no delay in the photocurrent response. That is, if we supply an incident light signal with frequency above the threshold to the phototube, we would expect the corresponding photocurrent signal to with a delay of much lower order than the classical one.

In the classical case, if we suppose the light signal is being supplied with some power P, given the electrons on the metal are uniformly spaced with some distance d, we can assume each electron absorbs the signal at a constant rate in a square of length d centered around it. Since the intensity of the light incident on each square is just $L = P/A$, we end up getting that power supplied to each individual electron is just $P_e = Id^2 = Pd^2/A$. The time required T for this input rate of energy to supply energy for the electron to leave the metal satisfies $P_eT = E_0$, so the delay for the current to start flowing is approximately:

$$T = \frac{AE_0}{Pd^2} \tag{3}$$

which we can calculate as the classical theoretical delay time in our lab, and compare with the experimental result [1]. If our finding is on a much smaller order of magnitude than this delay time, the semiclassical model would seem more reasonable. Together, these measurements will let us reproduce the results of Philip Lenard's analoguous experiment and the corresponding conclusions made.

3 Procedure and Methods

For this experiment, various light sources were positioned to be incident into a phototube, composed of a cathode and anode inside a closed container with a single hole designated for the lights. To minimize any outside light exposure or intensity reduction of the source, we ensured that the light source was kept very close to the hole. Note that these lights were LEDs connected to a power source.

The cathode and anode were connected to a circuit, composed of several key components in a box. Particularly, there was a terminal for which the voltage of the photocurrent flowing to the anode could be measured with a voltmeter added in parallel to a 100 kΩ resistor. There was another

section of the circuit that will apply the opposing potential, with a potentiometer powered by a battery that can be adjusted by a knob. Another terminal was placed over this, to measure the voltage applied by the potentiometer. This setup is outlined in Figure 1.

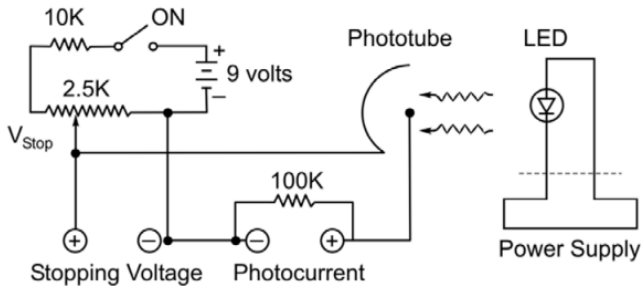

Figure 1: The photoelectric effect experiment setup as described. See [1] for more details.

We performed three different experiments using this equipment. First, we used 8 different wavelength (and so frequency) LEDs (shown in 2 (a)) of the same intensity, ranging from ultraviolet to infrared (see section 5.1). The wavelengths designated by the equipment manual were given as 390, 455, 505, 535, 590, 615, 640, and 935 nm.

We then measured the stopping voltage required to negate the photocurrent voltage for each wavelength, by adjusting the potentiometer knob until the photocurrent voltage vanished.

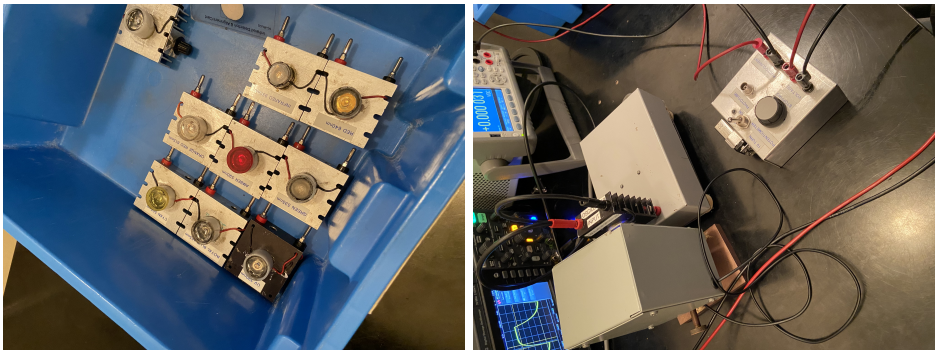

(a) Image of various LEDs. (b) Image of experimental apparatus.

Figure 2: Various LEDs for the experiment in (a), along with the experiment apparatus in (b).

We found that the photocurrent voltage fluctuated randomly in the 10^{-1} mV range, so we took any readings as 0 V if all decimal digits up to the 4th vanish. The potentiometer knob was very sensitive to slight motions, so we made sure to use very small adjustments to fine tune the stopping voltage for maximum accuracy. When making stopping voltage readings, we also had to wait a moment for the potentiometer knob to settle, so none of the residual vibrations change it. There was a similar fluctuation that arises in the stopping voltage readings as with the photocurrent readings, suggesting noise in the circuit due to other unknown factors independent of the current flowing through it.

For the second part, we used a diode of single frequency but with 4 intensity settings. Note that there were arbitrary units on the intensity setting, but they monotonically increased with each setting, so any general description of trends in intensity could still be measured. We then measured the photocurrent voltage generated for each intensity setting–without any opposing potential applied–and then the stopping voltage required for each intensity setting, independently of each other.

For the last component of the experiment, we connected an oscilloscope to the photocurrent voltage terminal and to an oscillator-driven LED incident into the phototube. We then fed a generated 1 kHz frequency square wave into the LED so it produced an oscillating light signal, which then should and did produce a slightly damped and delayed photocurrent response. The oscilloscope then measured and displayed this over each sampling period as given in Figure 3.

The oscilloscope also estimated the standard rise time of the filtered wave in every sampled period, corresponding to the time required for the pulse to move from 10% to 90% of its effective amplitude. This is a good estimate of the delay time, as the square wave source provides an instant spike at $t = 0$, which then means that the time it takes for the response to spike is the delay.

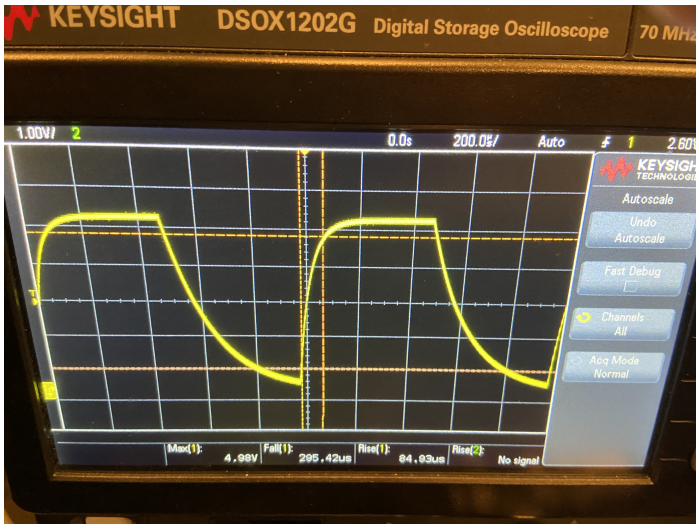

Figure 3: Oscilloscope generating a square wave fed into the oscillator-driven LED, producing a photocurrent response as the wave shown in this image.

4 Constants and Uncertainties

The uncertainties of the constants we will be using in our analysis are standard. In the case of the voltage readings in both the photocurrent and stopping voltage, recall that the random fluctuations were of order 10^{-1} mV. Hence, we could measure to a degree of precision up to the 4th digit, so we assign a standard digit uncertainty of ± 0.0001 V to our voltage measurements.

In the case of the frequencies, we are given the wavelengths of the diodes we use for the first experiment, as mentioned in the last section to be 390 ± 40, 455 ± 40, 505 ± 30, 535 ± 30, 590 ± 10,

615 ± 10, 640 ± 10, and 935 ± 10 nm with the uncertainties included. These are given in the lab manual, detailing them as the spectral widths of diodes' light wavelength ranges, and hence behave as if they were uncertainties for the specified wavelengths [1].

During the experiment, we use frequencies instead of wavelengths of the incident light, which are compute from each wavelength λ as $f = c/\lambda$, where $c = 2.99 \cdots \times 10^8$ m/s^2 is the speed of light, which is an exact value according to the NIST database of constants [3].

We can compute the uncertainty on f using the standard uncertainty propagation for inversion [5]. That is, we can calculate:

$$\Delta f = f\Delta\lambda/\lambda = \frac{c\Delta\lambda}{\lambda^2} \tag{4}$$

since the relative uncertainties after inversion and multiplication by an exact value are the same. The intensity setting has arbitrary units without any specified uncertainties on the equipment, so if we assume that the setting is precise up to $\pm 10\%$ of its range, we expect a standard uncertainty of $\pm 10\%$. Note that there is no other justification for this without the premise that the diode's intensity setting is reasonably precise in a statistical sense (i.e., its value hovers like a standard Gaussian with most of its peak contained within $\pm 10\%$).

When fitting our data, we plug in the uncertainty on the data into the curve fitting method of Python, which then outputs the fitted parameters with the corresponding computed uncertainties. When fitting particularly the relationship between stopping voltage and frequency as $V_s = mf + b$, if we assume the semiclassical model to be true, we know that $m = h/e$, where $e = 1.60 \times 10^{-19}$ C is the electron charge and h is Planck's constant. We hence can compute a value for Planck's constant $h = em$, and as e is an exact value [2], we get that:

$$\Delta h = e\Delta m \tag{5}$$

as the uncertainty just scales by the exact value due to standard uncertainty propagation [5]. Likewise, we recall that $b = -E_0/e$ for the phototube's work function E_0, so we can calculate $E_0 = -eb$ and:

$$\Delta E_0 = e\Delta b \tag{6}$$

We also know that the threshold frequency $f_0 = E_0/h$, so its standard uncertainty is via error propagation of products:

$$\Delta f_0 = \frac{E_0}{h}\sqrt{(\frac{\Delta E_0}{E_0})^2 + (\frac{\Delta h}{h})^2} \tag{7}$$

Finally, when estimating the classical delay time, we assume an input power value of the oscillator-driven diode of $P = 6.0 \times 10^{-5}$ W in accordance with the lab manual [1], with a $\pm 0.1 \times 10^{-5}$ W standard uncertainty based on the degree of precision. We also are assuming the surface area of the phototube's cathode to be $A = 3.23 \times 10^{-4}$ m, with standard uncertainty $\pm 0.01 \times 10^{-2}$ m. The electron spacing $d = 3 \times 10^{-10}$ m as well, for which we have a standard uncertainty of $\pm 1 \times 10^{-10}$ m to maintain consistency. Note that these uncertainties are not specified in the lab manual, so we are assuming the values given are precise to the digit.

We can hence compute the total uncertainty of the classical delay time as [5]:

$$\Delta T = \frac{AE_0}{Pd^2}\sqrt{(\frac{\Delta A}{A})^2 + (\frac{\Delta E_0}{E_0})^2 + (\frac{\Delta P}{P})^2 + 2(\frac{\Delta d}{d})^2} \tag{8}$$

The measurement of the actual delay time–given by the standard rise time of the oscilloscope–fluctuated by ± 3 μs over the sampling about $T_a = 85$ μs. Hence, this will be our standard uncertainty for our actual delay time.

5 Results and Analysis

Using our aforementioned theory and methods paired with the uncertainty propagation, we can proceed with discussing the results of the three sections of our lab.

5.1 Frequency with Stopping Voltage

During the first experiment, we found that for the last data point, corresponding to 935 nm wavelength light source, produced no photocurrent and so required no stopping voltage. This suggests instantly that there is a positive x intercept in the V_s-f relationship, giving some justification for assuming the semiclassical model when fitting this relation.

Particularly, we fit our data to Equation (1). However, noting that the linear relation is only valid for $f > f_0$, fitting with our last point (corresponding to the lowest frequency) might reduce the accuracy to the real fit, as V_s should be flat in that range. Hence, we decided to omit that point to reduce any errors in the fitting, given in Figure 4.

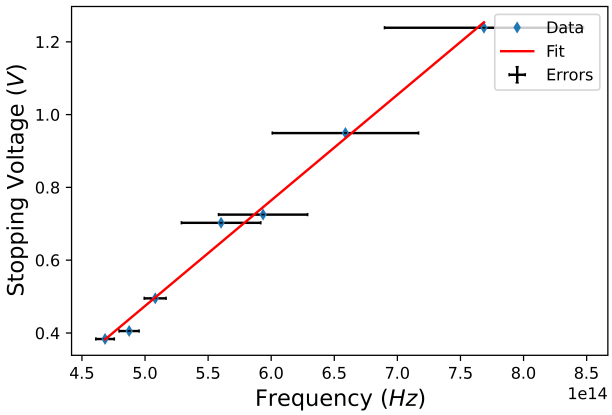

Figure 4: Graphs of the measured stopping voltages varied with the frequency of the incident light signal without the lowest frequency data point, fitted to linear relation. The fit parameters are $m = (2.9017 \pm 0.0003) \times 10^{-15}$ VHz^{-1} and $b = -0.9771 \pm 0.0002$ V.

The error bars are extremely small for the stopping voltages, in relation to their range of values, as seen for the y error bars in the graphs. Because of this, the chi squared test would not effectively assess how well this fits, since it does not account for the errors in the x axis and division by the relatively small errors would make it blow up unreasonably. This also makes the error estimates on the fit parameters exceedingly small, which will contribute later to a lack of a sufficiently large uncertainty value on our computed values.

Visually, the fit looks like it agrees relatively well with the data within the range of errors. To check this more rigourously, we plot the residuals in Figure 5. In either case, we see that they fluctuate near 0 in a relatively symmetric manner. As a remark, if the fit is good, we expect the residuals to be completely independent of each other–that is, they would be distributed around 0 as a normal distribution.

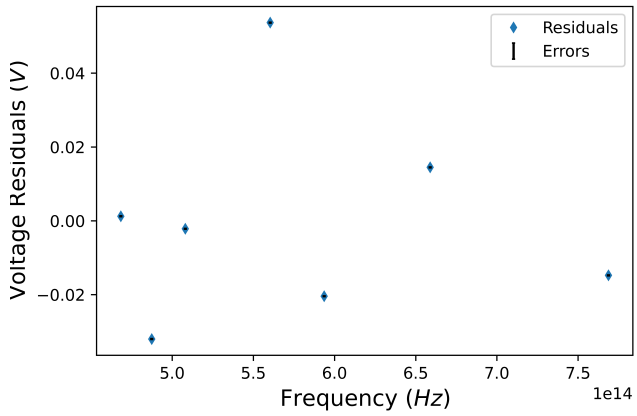

Figure 5: Graphs of the residuals of the stopping voltage vs. frequency fit made in Figure 4. Although there isn't enough data to make any straight-forward conclusion, the residuals seem like they do not depend on each other, although the error bars are again very small.

Normally, we would plot the residuals in a histogram to see if this was the case. However, this only works for large samples of data–in our case, only 7 data points could resemble nearly any distribution's shape, if any shape could even be discerned from the limited bin sizes and range on such a small pool of data. Just looking at this and the plot by itself with the x error bars, one could judge that the relation is indeed linear, giving more confidence to the semiclassical model.

Using these values of m and b, we can calculate Planck's constant as $h = em$ with uncertainty as in equation (5) given in the previous section. This produces a value of $h = (4.6491 \pm 0.0006) \times 10^{-34}$ Js. Likewise, we can compute $E_0 = eb$ with the uncertainty given by equation (6), as $E_0 = (1.5655 \pm 0.0003) \times 10^{-19}$ J.

Together, we can compute the threshold frequency $f_0 = E_0/h$ with uncertainty from equation (7), which gives us $f_0 = (3.2850 \pm 0.0004) \times 10^{14}$ Hz, as the parameters describing the photoelectric effect for our phototube, if we assume our semiclassical model.

For comparison, the accepted exact value for Planck's constant is $h = 6.62 \times 10^{-34}$ Js [4], which has a percent error from our calculated value of around 30%–much larger than the projected uncertainty of h from the fit, although still within the same order of magnitude. To be clear, this uncertainty does not include any contributions from the visible uncertainties in the frequency widths of the lights used, since the fit only takes into account y errors. A better alternative in hindsight might have been to fit with the axes swapped, or to use a fitting tool that also incorporates x axis uncertainties to more accurately reflect the error widths. The large discrepancy might also suggest that there are additional systenatic errors that we have not accounted for in the methods of performing the

experiment.

5.2 Intensity with Stopping Voltage and Photocurrent Voltage

For the second experiment, we are plotting the relationship between the intensity setting with either the photocurrent or stopping voltage separately. Since we have such a limited data set of only 4 points and do not know the precise units or scaling of the intensity setting, we cannot make any real judgements of the relationship other than just the direction it seems to be going, which we can estimate by fitting it to a line. In the case of the photocurrent voltage, this is actually justified, since we expect a linear trend that passes through the origin, as discussed previously. In the case of the stopping voltage, we expect no changes over time. However, note that this fit may not be very good, considering that the y uncertainties seem to be insufficient in describing the actual resolution of the measurement, as mentioned in the first experiment.

It suffices to just look for general qualitative behaviour that is somewhat sensible in the fit. That is, we expect the intercept of the photocurrent fit to be close to 0, while the slope of the stopping voltage fit instead should be close to 0. The plot for the photocurrent voltage is given in Figure 6, while that of the stopping voltage is in Figure 7, where we denote i as a placeholder unit for the intensity setting.

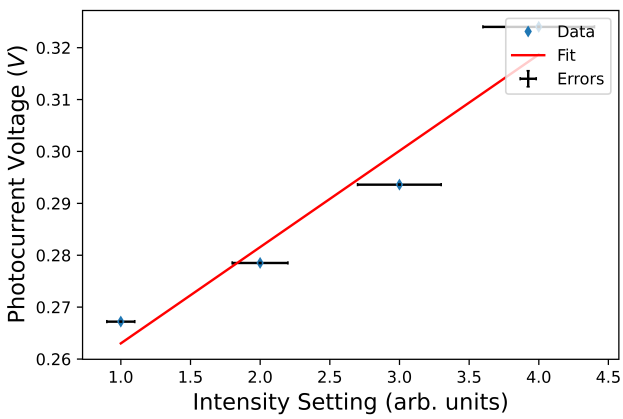

Figure 6: Graph of the intensity setting with the corresponding photocurrent voltage, fitted to a line. The fitting parameters are $m = (1.854 \pm 0.004) \times 10^{-2}$ Vi^{-1} and $b = (2.444 \pm 0.001) \times 10^{-1}$ V.

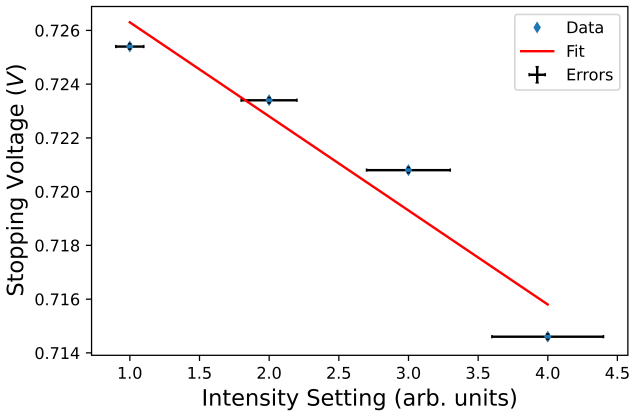

Figure 7: Graph of the intensity setting with the corresponding stopping voltage, fitted to a line. The fitting parameters are $m = (-0.350 \pm 0.004) \times 10^{-2}$ Vi^{-1} and $b = (7.300 \pm 0.001) \times 10^{-1}$ V.

We observe that the order of magnitude of the uncertainties for the slopes and intercepts of both the photocurrent and stopping voltage remain the same, while that of the slope going from the photocurrent to the stopping voltage is around 1/5 and vice versa for the intercept. This because the range in which the stopping voltage varies is much smaller than that of the photocurrent. Even so, it seems that the photocurrent has a nonzero intercept, while the stopping voltage has a clear downwards trend without considering any other errors.

The first observation can be explained by the arbitrariness of the intensity setting axis. It is entirely possible that the intensity settings corresponds really to just a shifted scale of intensity measurements, the shift of which would obviously generate a fictitious intercept which does not normally exist. This could also possibly be the reason why the trend of the data in both graphs seems to have curvature like a quadratic or an exponential, corresponding exactly to the inhomogeneity of the scaling of the intensity axis in the intensity settings.

The second result is more obscure, as it neither agrees with the classical result of an increasing stopping voltage, or the semiclassical result of a static stopping voltage. To be fair, it much closer to the semiclassical prediction, considering that it is not even increasing and that it is decreasing at such a marginal scale–recall the scale that the stopping voltage changed on in the first experiment was on order of 1 V, while here it is around 0.01 V. This can be attributed to systematic error from the light source itself, possibly from the source's frequency range shifting slightly as the intensity increases due to the internal mechanism producing the light, which might cause the very slight drop in stopping voltage and possibly even the qualitative curvature in both data sets. In any sense, this still falls much closer in agreement with the semiclassical model

5.3 Delay Time Measurement

On the topic of the last experiment, recall that the actual delay time we measured was $T_a = (8.5 \pm 0.3) \times 10^{-5}$ s. If we use the value for the work function that we computed from our previous analysis, we can compute the classical expected delay time using equation (3) from the introduction, with the uncertainty propagation from the last section with equation (8), as around $T = 0.9 \pm 0.3$ s

up to the highest digit of the uncertainty.

Clearly, this delay is much higher than the one we observed, which is an order of magnitude 10^5 smaller, even after considering the most liberal estimates of variation within the uncertainty widths. This discrepancy gives much more credibility to the semiclassical model, which predicts very small delay times in the photocurrent, and is another good marker for why the classical theory does not properly explain this effect.

6 Extension

To improve on the first experiment, it may help to reduce the larger error bars on the x axis in each experiment, or at least incorporate them into the uncertainty somehow. As an alternative, we could also have fitted the inverted relationship, which would have accounted for the more significant uncertainties in the experiment and so would have made the calculations more consistent.

For the second experiment, having access to a much more precise instrument for varying intensity over a larger range of values would make it much easier to find the real shape of its relationship to the photocurrent voltage and stopping voltage. Paired with more specific calculations using formulae from the semiclassical and classical models, we would've been able to verify much more accurately how well either of them fit to the data.

In the case of our final experiment, the theoretical computation was paired with a lot of assumptions in the values and uncertainties in the electron spacing, area of the cathode, and power output of the irradiating light signal. If these measurements were made more precisely in the advent of the experiment, with precise measuring tools, although it would not have changed the result of the experiment–considering the order of magnitude would still be the same–it would more accurately reflect the actual discrepancy while also giving us a metric for judging when the semiclassical result in other experiments might apply to it more conveniently.

7 Conclusion

All in all, we were able to successfully reproduce Lenard's experiment on the photoelectric effect. Particularly, we measured the relationship between the frequency of the light incident on a phototube's cathode and the stopping voltage required to negate the photocurrent response, in which we observed that there was indeed a nonzero incident frequency for which no photocurrent was produced, suggesting the semiclassical model might apply. Fitting this with equation (1) let us compute values for Planck's constant $h = (4.6491 \pm 0.0006) \times 10^{-34}$ Js, the work function of the cathode's metal $E_0 = (1.5655 \pm 0.0003) \times 10^{-19}$ J, and the frequency threshold $f_0 = (3.2850 \pm 0.0004) \times 10^{14}$ Hz. A qualitative analysis of the fit and the residues, along with agreement of our measured Planck's constant with the actual value in the order of magnitude–considering the uncertainties were underestimated–was suggestive of the validity of the semiclassical theory of this effect.

On top of this, the relation between the intensity of the incident light and stopping voltage indeed exhibited an effect better explained by the semiclassical model than the classical: the stopping voltage changed marginally while the intensity of the incident light was varied, and the marginal change was a decrease rather than an increase in voltage. This, as well as the fact that the photocurrent also increased in a manner consistent with the model together gives us more motivation

for why the semiclassical model might actually be correct.

Last but not least, the delay time of the photocurrent response was measured by subjecting the cathode to a square wave light signal and then measuring the standard rise time of the response voltage, giving a value of $T = (8.5 \pm 0.3) \times 10^{-5}$ s. Comparing this to a theoeretically calculated classical value for what the delay time should be as $T_a \approx 0.9 \pm 0.3$ s, we saw that the actual delay was much smaller than what would be expected if the classical theory were true. This significant order of magnitude of 10^5 between the two is enough to decide that the classical model is not enough to sufficiently describe the photoelectric effect. Since the semiclassical model that Einstein proposed coincides much closer to these observations–even predicting a near instant response–with the other results lets us conclude that it is a much better representation of the behaviour of the physical elements in this effect and possibly in other similar settings of phenomena.

This reasoning offers a natural gateway to the quantization of electromagnetism and classical mechanics, which is exactly the path that modern physics took after this effect–among others–was dissected and studied further. This provides motivation for such a path for the student as they study physics at this level and beyond.

References

[1] Josiah Sinclair (2017), "The Photoelectric Effect." Last accessed 19 March 2023 at `https://www.physics.utoronto.ca/~phy293lab/photoelectric%20effect.pdf`.

[2] *NIST Reference on Constants, Units and Uncertainty* (2019), "elementary charge." Last accessed 19 March 2023 at `https://pml.nist.gov/cgi-bin/cuu/Value?e`.

[3] *NIST Reference on Constants, Units and Uncertainty* (2019), "speed of light in vacuum." Last accessed 19 March 2023 at `https://pml.nist.gov/cgi-bin/cuu/Value?c`.

[4] *NIST Reference on Constants, Units and Uncertainty* (2019), "Planck constant." Last accessed 19 March 2023 at `https://pml.nist.gov/cgi-bin/cuu/Value?h`.

[5] Vern Lindberg (2000), "Uncertainties and Error Propagation." Last accessed on 18 March 2023 at `https://www.geol.lsu.edu/jlorenzo/geophysics/uncertainties/Uncertaintiespart2.html`.

[6] David Hanson et al (2022), "2.3: Photoelectric Effect." Last accessed 19 March 2023 at `https://chem.libretexts.org/Bookshelves/Physical_and_Theoretical_Chemistry_Textbook_Maps/Book%3A_Quantum_States_of_Atoms_and_Molecules_(Zielinksi_et_al)/02%3A_Foundations_of_Quantum_Mechanics/2.03%3A_Photoelectric_Effect`.